Vehicle Platoon Control with Virtual Path Constraints

Jianwei Sun and Rajan Gill

Abstract— This paper studies distributed platoon control with virtual path constraints. Using transverse feedback linearization, the control approach decouples the platoon's dynamics into components tangential and transversal to the path. A platoon controller exclusively in the tangential subsystem controls the platoon's formation tangentially along the path, while a feedback control law in the transversal component stabilizes the platoon to remain on the path. As an application of the theory, a human-robot interaction experiment is performed on a platoon of quadrotors. The platoon leader implements an admittance controller, which allows the platoon to respond to human-applied forces. The path constraints limit the platoon's movement to only be along the path, ensuring safety to the interacting human.

I. INTRODUCTION

This paper explores a distributed control methodology for a path-constrained robotic platoon. A platoon is a single file queue of robots in which each robot follows its preceding neighbor, with the foremost robot leading the trajectory of the platoon. The path constraints limit the platoon's range of motion to only be tangential to a given, virtual path in three dimensional space. *Transverse feedback linearization* (TFL) [1–5] is used to separate the control of the platoon tangentially along the path, from stabilization of the platoon onto the path. As a result, the dynamics are decoupled, which allows for independent controllers.

The control methodology builds upon the works of [1–6] by extending path-constrained control to a robotic platoon. The path-constrained approach can be more advantageous than trajectory-tracking methods, such as those presented in [7, 8], because of better regulation of spatial errors transversal to the path, time-invariance of the controller, and applicability to general mechanical systems, such as highway vehicles, robotic arms, and flying robots as long as their dynamics satisfy certain TFL assumptions [2–4, 9]. The path can also be selected to satisfy the particular application's safety requirements, as long as an appropriate diffeomorphism is defined [1–4]. Previous literature has explored different classes of paths, such as spline-interpolated paths [1, 10], elliptical paths [2], and paths containing segments without curvature [11].

While platoons have been studied extensively in literature [12–19], little has been investigated in the area of platoon control with virtual path constraints. Traditionally, platoon control is applied to highway vehicular systems that assume

straight roads and thus do not consider transversal spatial errors [12, 13, 18]. However, this paper extends platoon control using path constraints, which enable curved paths and safety guarantees through regulating transversal errors.

Furthermore, *human-robot interaction* (HRI) with a quadrotor platoon is explored as an application of the proposed path-constrained platoon control. An admittance controller is implemented on the platoon leader to allow a human to interact with the platoon, while the virtual path constrains the platoon and thus guarantees safety to the human. While [20] studied human interaction with a quadrotor via admittance control and [19] studied human interaction with a platoon using gradient tracking, neither did so in context of virtual path constraints.

Path-following via TFL is combined with platoon control in the tangential dynamics to result in a distributed control scheme that allows a platoon to satisfy virtual path constraints. Additionally, the control methodology was verified through a HRI experiment enabled by path-constrained admittance control on the platoon leader. To our knowledge, neither undertaking had previously been explored in literature.

This paper is organized as follows: Section II describes the TFL theory for a path-constrained platoon. Section III then describes application details, such as the quadrotor model, virtual path, and admittance control on the platoon leader. Finally, Section IV describes experimental results and Section V concludes the paper.

II. PATH-CONSTRAINED PLATOON CONTROL

This section presents the general path-constrained platoon control methodology based on results from [1–5, 21], feedback linearization theorems from [9], and platoon-control design from [12, 13]. Consider a platoon consisting of identical robots with arbitrary initial positions. Let each platoon member be indexed by the superscript $^{(i)}$, where $i = 0$ corresponds to the platoon leader. Let the dynamics of the ith platoon member be

$$\dot{x}^{(i)} = f(x^{(i)}) + g(x^{(i)})u^{(i)}, \qquad (1)$$

where $x^{(i)} \in \mathbb{R}^n$ is the ith member's state, $u^{(i)} \in \mathbb{R}^m$ is the vector of control inputs, and $f(\cdot) : \mathbb{R}^n \to \mathbb{R}^n$, $g(\cdot) : \mathbb{R}^n \to \mathbb{R}^{n \times m}$ are smooth functions. Furthermore, let the output of the robots' dynamics be

$$y^{(i)} = h(x^{(i)}), \qquad (2)$$

where $h(\cdot) \in \mathbb{R}^n \to \mathbb{R}^m$ is a smooth function. It is assumed that the system is square in that the number of inputs is equal to the number of outputs, and that $m \geq 2$.

Now consider a given virtual path in the output space parameterized by a smooth curve, $\sigma(\cdot) : \mathbb{R} \to \mathbb{R}^m$. If the path is closed, then $\sigma(\theta + \theta_L) = \sigma(\theta)$ for some finite θ_L. Assume that the path is an embedded submanifold of $\mathbb{R}^m$ with dimension 1 and that there exists a smooth function $s(\cdot) : \mathbb{R}^m \to \mathbb{R}^{m-1}$ such that 0 is a regular value and that $\sigma(\mathbb{R}) = s^{-1}(0)$ [4, 5, 10, 11]. Define the path as $\gamma := s^{-1}(0)$. Furthermore, let Γ^* with $\dim(\Gamma^*) > 0$ be the largest invariant set contained within the submanifold $(s \circ h)^{-1}(0)$, which is also called the lift of γ to $\mathbb{R}^n$ [1, 4, 5]. It is assumed that Γ^* is non-empty. Additionally, assume that $g(\cdot)$ has rank m in a neighbourhood U of Γ^*. From literature, Γ^* is called the *path-following manifold* [1–5].

The objective of path-constrained platoon control is to design a feedback control scheme that attracts and constrains a platoon to the virtual path. The platoon's trajectory along the path is determined by the platoon leader, which implements a controller specific to the application. These requirements can be more formally expressed as the following objectives.

Objective 1 (Decoupling): Find a transformation $T(\cdot) : x^{(i)} \to \mathrm{col}(\eta^{(i)}, \xi^{(i)})$ defined on U for each platoon member, $i = 0, 1, \ldots$, that decouples the robot's dynamics to those tangential to the path, $\dot{\eta}^{(i)}$ (also known as the *tangential subsystem*), and those transversal to the path, $\dot{\xi}^{(i)}$ (also known as the *transversal subsystem*) [2, 4, 5]. Additionally, let the tangential and transversal subsystems be independently controlled by auxiliary control variables, $v_{\parallel}^{(i)}$ and $v_{\pitchfork}^{(i)}$, respectively, and find the mapping from $v^{(i)} = \mathrm{col}(v_{\parallel}^{(i)}, v_{\pitchfork}^{(i)})$ to $u^{(i)}$. The goal of having each subsystem's output only be affected by a corresponding set of inputs is known as the *Noninteracting Control Problem* of [9].

Objective 2 (Platoon Formation): Let the platoon controller exist solely in the tangential subsystem. Find a control law for $v_{\parallel}^{(i)}$ that ensures each follower, i, where $i = 1, 2, \ldots$, maintains a given constant relative spacing $d_{\mathrm{ref}}^{(i)}$, measured tangentially along the path, from its preceding member, $i-1$. Note that the platoon control law is not applicable to the leader, $i = 0$.

Objective 3 (Path Attractiveness): For any initial condition $x_0^{(i)}$ within U and for every member of the platoon, $i = 0, 1, \ldots$, the closed loop control law should drive the robot's position to the path asymptotically: $\inf_{p \in \gamma} \| y^{(i)}(t) - p \| \to 0$ as $t \to \infty$.

Objective 4 (Path Invariance): The closed loop control law should ensure that each platoon member, $i = 0, 1, \ldots$, remains on the path if it starts on it. In other words, if $y^{(i)}(0) \in \gamma$, then $y^{(i)}(t) \in \gamma, \ \forall \ t > 0$.

TFL is well-suited to satisfy these objectives for the path-constrained platoon because it decouples the control of the tangential and transversal subsystems [2, 4, 5]. Path attractiveness and invariance can be achieved by an appropriately-designed feedback control law in the transversal subsystem [5]. In the tangential subsystem, a platoon control law similar to the one in [12] will be implemented to achieve the desired platoon member spacing requirements.

The approach described above requires a few extra definitions to be made. Let

$$\varpi(y^{(i)}) := \int_0^{\arg\inf_\theta \| y^{(i)} - \sigma(\theta) \|} \left\| \frac{\mathrm{d}\sigma(\tau)}{\mathrm{d}\tau} \right\| \mathrm{d}\tau + kL, \quad (3)$$

where $\varpi(\cdot) : \mathbb{R}^m \to \mathbb{R}$ is a mapping from a platoon member's position to the arc-length of the closest point on the path. Note that if the path is closed and has a closed arc-length of L, then the mapping is unwrapped by the kL term, where $k \in \mathbb{Z}$ counts the number of full cycles already made around the path by the robot. Otherwise $kL = 0$ for non-closed paths.

Now using $s(\cdot)$ and $\varpi(\cdot)$, define a virtual output of system (1) with real output (2) as:

$$\hat{y}^{(i)} := \begin{bmatrix} \pi(x^{(i)}) \\ \lambda(x^{(i)}) \end{bmatrix} := \begin{bmatrix} \varpi \circ h(x^{(i)}) \\ s \circ h(x^{(i)}) \end{bmatrix}. \quad (4)$$

Let r_j be the relative degree as defined in [9] of the jth element of $\hat{y}^{(i)}$. Note that r_j does not depend on (i) as all robots in the platoon have the same dynamics. Assume that

$$\sum_{j=1}^m r_j = n \quad (5)$$

on U, so that system (1) with virtual output (4) is feedback linearizable [2–5, 9]. Note that the validity of this assumption is determined by [5, Theorem 3.2]. Then, by taking the time derivative of each element of $\hat{y}^{(i)}$ by the number of times corresponding to the relative degree r_j and stacking the results, the following is obtained:

$$\begin{bmatrix} d^{r_1}\hat{y}_1^{(i)}/dt^{r_1} \\ d^{r_2}\hat{y}_2^{(i)}/dt^{r_2} \\ \vdots \\ d^{r_m}\hat{y}_m^{(i)}/dt^{r_m} \end{bmatrix} = \begin{bmatrix} L_f^{r_1} \pi(x^{(i)}) \\ L_f^{r_2} \lambda_1(x^{(i)}) \\ \vdots \\ L_f^{r_m} \lambda_{m-1}(x^{(i)}) \end{bmatrix} +$$

$$\begin{bmatrix} L_{g_1} L_f^{r_1-1} \pi(x^{(i)}) & \cdots & L_{g_m} L_f^{r_1-1} \pi(x^{(i)}) \\ L_{g_1} L_f^{r_2-1} \lambda_1(x^{(i)}) & \cdots & L_{g_m} L_f^{r_2-1} \lambda_1(x^{(i)}) \\ \vdots & \ddots & \vdots \\ L_{g_1} L_f^{r_m-1} \lambda_{m-1}(x^{(i)}) & \cdots & L_{g_m} L_f^{r_m-1} \lambda_{m-1}(x^{(i)}) \end{bmatrix} u^{(i)}$$

$$:= \begin{bmatrix} D_1(x^{(i)}) + E_{1,1:m}(x^{(i)})u^{(i)} \\ D_2(x^{(i)}) + E_{2,1:m}(x^{(i)})u^{(i)} \\ \vdots \\ D_m(x^{(i)}) + E_{m,1:m}(x^{(i)})u^{(i)} \end{bmatrix}$$

$$:= D(x^{(i)}) + E(x^{(i)})u^{(i)},$$
$$:= \mathrm{col}(v_{\parallel}^{(i)}, v_{\pitchfork}^{(i)})$$
$$:= v^{(i)}, \quad (6)$$

where $L_b^a c(x)$ is the ath Lie derivative of $c(x)$ along b. $L_b^a c(x)$ is recursively defined as $L_b^a c(x) = L_b L_b^{a-1} c(x)$, where $L_b c(x) = \frac{\mathrm{d}c(x)}{\mathrm{d}x} b(x)$. The matrix $E(x^{(i)})$ is known as the *decoupling matrix* for the MIMO system [5, 9]. Note that $E(x^{(i)})$ is non-singular on U [9]. Equation (6) is then a chain

of integrators with vector control input $v^{(i)}$. Through defining $\alpha(x^{(i)}) := -E^{-1}(x^{(i)})D(x^{(i)})$ and $\beta(x^{(i)}) := E^{-1}(x^{(i)})$, the auxiliary control input maps to the original control input through

$$u^{(i)} = \alpha(x^{(i)}) + \beta(x^{(i)})v^{(i)}. \tag{7}$$

By defining the diffeomorphism $T(\cdot) : x^{(i)} \to (\eta^{(i)}, \xi^{(i)})$ as

$$\begin{bmatrix} \eta^{(i)} \\ \xi^{(i)} \end{bmatrix} := \begin{bmatrix} \mathrm{col}(\pi, \dots, L_f^{r_1-1}\pi)(x^{(i)}) \\ \hline \mathrm{col}(\lambda_1, \dots, L_f^{r_2-1}\lambda_1)(x^{(i)}) \\ \vdots \\ \mathrm{col}(\lambda_{m-1}, \dots, L_f^{r_m-1}\lambda_{m-1})(x^{(i)}) \end{bmatrix}, \tag{8}$$

the path-following manifold in the new coordinates is $T(\Gamma^*) = \{(\eta^{(i)}, \xi^{(i)}) : \xi^{(i)} = 0\}$, for any $i = 0, 1, \dots$. Furthermore, the dynamics in the new coordinates are in Brunowský normal form [2, 5]:

$$\dot{\eta}^{(i)} = A^{\parallel}\eta^{(i)} + B^{\parallel}v_{\parallel}^{(i)}, \tag{9}$$

$$\dot{\xi}^{(i)} = A^{\pitchfork}\xi^{(i)} + B^{\pitchfork}v_{\pitchfork}^{(i)}, \tag{10}$$

where $(A^{\parallel}, B^{\parallel})$ and (A^{ξ}, B^{ξ}) are controllable. Equation (9) describes the dynamics that are tangential to the path, and is therefore defined as the *tangential subsystem* [4, 5]. Likewise, equation (10) describes transversal dynamics and is defined as the *transversal subsystem* [4, 5]. These results satisfy **Objective 1**.

Stabilizing the origin of the transversal subsystem ensures that the robot's position remains on the path-following manifold [4, 5]. This can be accomplished by an appropriate feedback control law, such as $v_{\pitchfork}^{(i)} = -K^{\pitchfork}\xi^{(i)}$ so that $A^{\pitchfork} - B^{\pitchfork}K^{\pitchfork}$ is Hurwitz. This controller would drive trajectories towards $\xi^{(i)} = 0$ for all platoon members, satisfying **Objective 3**. Since the origin of the transversal subsystem can be made a stable equilibrium by the closed loop controller, **Objective 4** is also satisfied.

In the tangential subsystem, the distributed platoon controller regulates the positions, $\eta^{(i)}$, of each follower robot to track its constant reference spacing, $d_{\mathrm{ref}}^{(i)}$. Note that the platoon leader does not have any spacing requirements. Assume that each robot of the platoon can communicate its instantaneous tangential state $\eta^{(i)}$ and control input $v_{\parallel}^{(i)}$ to its immediate follower. Define $\delta^{(i)} := \eta^{(i-1)} - \eta^{(i)}$ as the ith robot's spacing state, where $i = 1, 2, \dots$, and $q^{(i)} := v_{\parallel}^{(i-1)} - v_{\parallel}^{(i)}$ as the ith robot's control input that accounts for the feed-forward control term from its preceding neighbour. Using equation (9), the dynamics of this system are

$$\dot{\delta}^{(i)} = A^{\parallel}\delta^{(i)} + B^{\parallel}q^{(i)}, \tag{11}$$

$$d^{(i)} := C^{\parallel}\delta^{(i)} := \begin{bmatrix} 1 & 0 & \dots \end{bmatrix}\delta^{(i)}, \tag{12}$$

where the system's output, $d^{(i)}$, is the physical spacing of the robot as shown in Fig. 1. The objective of platoon control is to make this spacing approach a desired $d_{\mathrm{ref}}^{(i)}$. An integral term is included in the controller for robustness to ensure zero steady state error:

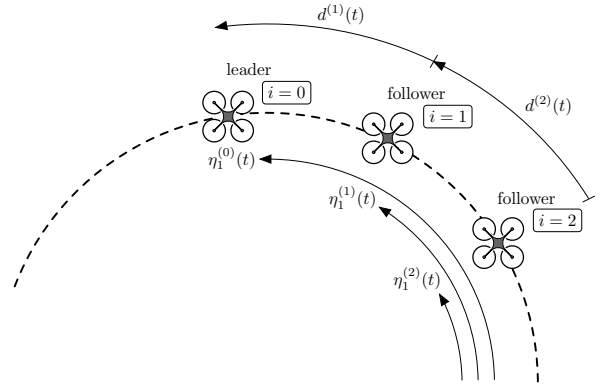$$\dot{\rho}^{(i)} := d^{(i)} - d_{\mathrm{ref}}^{(i)}. \tag{13}$$

Fig. 1. While constrained to the path-following manifold, the platoon is led by the leader. $d^{(i)}(t)$, $i = 1, 2, \dots$ is the spacing of the ith robot from its preceding neighbour. $\eta_1^{(i)}(t)$, $i = 0, 1, \dots$ is the absolute arc-length position of the ith robot along the path. Each robot in the platoon is able to communicate its instantaneous tangential state $\eta^{(i)}$ and control input $v_{\parallel}^{(i)}$ to its immediate follower.

Furthermore, let the robot's control be a state feedback:

$$q^{(i)} = -K_1^{\parallel}\delta^{(i)} - K_2^{\parallel}\rho^{(i)}, \tag{14}$$

and let the point $(\delta_{\mathrm{ss}}^{(i)}, q_{\mathrm{ss}}^{(i)}, \rho_{\mathrm{ss}}^{(i)})$ satisfy the steady state equations:

$$0 = A^{\parallel}\delta_{\mathrm{ss}}^{(i)} + B^{\parallel}q_{\mathrm{ss}}^{(i)}, \tag{15}$$

$$q_{\mathrm{ss}}^{(i)} = -K_1^{\parallel}\delta_{\mathrm{ss}}^{(i)} - K_2^{\parallel}\rho_{\mathrm{ss}}^{(i)}, \tag{16}$$

$$0 = C^{\parallel}\delta_{\mathrm{ss}}^{(i)} - d_{\mathrm{ref}}^{(i)}. \tag{17}$$

By defining $\zeta^{(i)} := \mathrm{col}(\delta^{(i)} - \delta_{\mathrm{ss}}^{(i)}, \rho^{(i)} - \rho_{\mathrm{ss}}^{(i)})$ and substituting equations (14) to (17) into equation (11), the closed loop dynamics become

$$\dot{\zeta}^{(i)} = \begin{bmatrix} A^{\parallel} - B^{\parallel}K_1^{\parallel} & -B^{\parallel}K_2^{\parallel} \\ C^{\parallel} & 0 \end{bmatrix}\zeta^{(i)}. \tag{18}$$

The platoon gains, $K_1^{\parallel}$ and $K_2^{\parallel}$, are then chosen such that the matrix describing the closed-loop system is Hurwitz. Stabilizing each follower's $\zeta^{(i)}$ state to the origin ensures that all outputs, $d^{(i)}$, $i = 1, 2, \dots$ track their reference spacing distances, $d_{\mathrm{ref}}^{(i)}$. This satisfies **Objective 2**.

III. EXPERIMENTAL SETUP

A. Quadrotor Dynamics

At the Flying Machine Arena (FMA) [22], the path-constrained platoon control scheme is implemented onto quadrotors due to their agility in three-dimensional space. A cascaded control structure, as shown in [1, Fig. 1], is used to simplify the control of each quadrotor. For each quadrotor, the structure consists of a body-rate controller, an attitude controller, and the path-constrained platoon controller designed in this paper. For more details about the design and implementation of the cascaded control structure, readers should refer to [1, 22].

Within certain bandwidth limits described by [22], the cascaded control structure allows each quadrotor to be modeled as a double integrator in each of the three inertial frame axes

[22]. The quadrotor's dynamics in the form of equation (1) are

$$\dot{x}^{(i)} = \begin{bmatrix} \mathbb{0}_{3\times3} & \mathbb{I}_{3\times3} \\ \mathbb{0}_{3\times3} & \mathbb{0}_{3\times3} \end{bmatrix} x^{(i)} + \begin{bmatrix} \mathbb{0}_{3\times3} \\ \mathbb{I}_{3\times3} \end{bmatrix} u^{(i)}. \quad (19)$$

In the FMA, every quadrotor's position is measured with a motion-tracking camera system [22], so the system's output in the form of equation (2) becomes

$$y^{(i)} = \begin{bmatrix} \mathbb{I}_{3\times3} & \mathbb{0}_{3\times3} \end{bmatrix} x^{(i)}. \quad (20)$$

B. Circular Path

To demonstrate the control scheme, a circle of radius R and parallel to the ground is chosen as the virtual path for its simplicity and non-triviality. The inertial frame coordinate system is defined with the origin at the circle's center.

In order to perform TFL, let $s(\cdot)$, as introduced in Section II, be a mapping of the system's output defined in equation (20) to the normal and binormal distances from the circle. Then, the virtual output functions $\pi(x^{(i)})$ and $\lambda(x^{(i)})$ are

$$\pi(x^{(i)}) = R\arctan\left(x_2^{(i)}/x_1^{(i)}\right) + kL, \quad (21)$$

$$\lambda(x^{(i)}) = \begin{bmatrix} \sqrt{\left(x_1^{(i)}\right)^2 + \left(x_2^{(i)}\right)^2} - R \\ x_3^{(i)} \end{bmatrix}, \quad (22)$$

where $L = 2\pi R$ is the circle's circumference and $k \in \mathbb{Z}$ is the number of full revolutions already made around the circle. Then, using equation (19), the diffeomorphism defined in equation (8) for this particular system is

$$T(x^{(i)}) = \begin{bmatrix} R\arctan\left(\frac{x_2}{x_1}\right) + kL \\ \frac{R(x_1\dot{x}_2 - x_2\dot{x}_1)}{x_1^2 + x_2^2} \\ \sqrt{x_1^2 + x_2^2} - R \\ \frac{x_1\dot{x}_1 + x_2\dot{x}_2}{\sqrt{x_1^2 + x_2^2}} \\ x_3 \\ \dot{x}_3 \end{bmatrix}_{x = x^{(i)}}. \quad (23)$$

Using $T(x^{(i)})$, the inertial frame coordinate system is transformed into the path coordinate system, $(\eta^{(i)}, \xi^{(i)})$, as shown in Fig. 2. The system dynamics in the path coordinates become decoupled chains of integrators:

$$\dot{\eta}^{(i)} = \begin{bmatrix} 0 & 1 \\ 0 & 0 \end{bmatrix} \eta^{(i)} + \begin{bmatrix} 0 \\ 1 \end{bmatrix} v_\parallel^{(i)}, \quad (24)$$

$$\dot{\xi}^{(i)} = \begin{bmatrix} 0 & 1 & 0 & 0 \\ 0 & 0 & 0 & 0 \\ 0 & 0 & 0 & 1 \\ 0 & 0 & 0 & 0 \end{bmatrix} \xi^{(i)} + \begin{bmatrix} 0 & 0 \\ 1 & 0 \\ 0 & 0 \\ 0 & 1 \end{bmatrix} v_\pitchfork^{(i)}. \quad (25)$$

The auxiliary control input, $v^{(i)} = \mathrm{col}(v_\parallel^{(i)}, v_\pitchfork^{(i)})$, is then mapped to the original control input, $u^{(i)}$, for $i = 0, 1, \ldots$
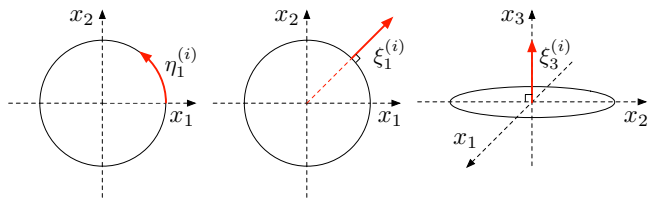

Fig. 2. The inertial frame coordinate system is transformed to the path frame coordinate system through diffeomorphism $T(x^{(i)})$. Note that $\eta_1^{(i)} \in \mathbb{R}$, where $i = 0, 1, \ldots$, is the unwrapped arc-length along the circular path.
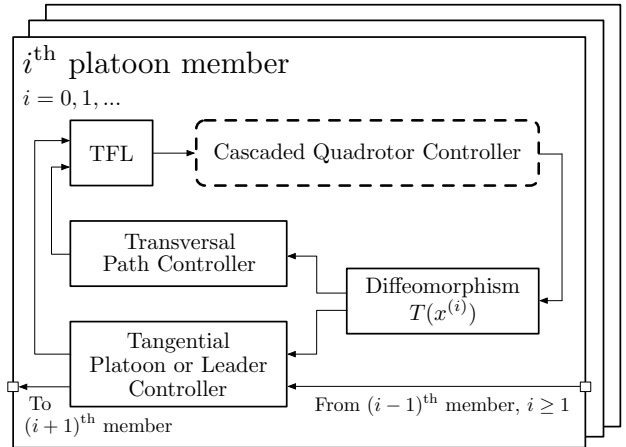

Fig. 3. The control methodology results in the overall distributed control scheme for a single quadrotor. The platoon leader implements an application-specific controller in its tangential subsystem, while the platoon followers implement the platoon control scheme.

through equation (7), where

$$\alpha(x^{(i)}) = \begin{bmatrix} \frac{2R(x_2\dot{x}_1 - x_1\dot{x}_2)(x_1\dot{x}_1 + x_2\dot{x}_2)}{(x_1^2 + x_2^2)^2} \\ \frac{(\dot{x}_1^2 + \dot{x}_2^2)(x_1^2 + x_2^2) - \frac{1}{2}(x_1\dot{x}_1 + x_2\dot{x}_2)}{(x_1^2 + x_2^2)^{\frac{3}{2}}} \\ 0 \end{bmatrix}_{x = x^{(i)}}, \quad (26)$$

$$\beta(x^{(i)}) = \begin{bmatrix} \frac{-Rx_2}{x_1^2 + x_2^2} & \frac{Rx_1}{x_1^2 + x_2^2} & 0 \\ \frac{x_1}{\sqrt{x_1^2 + x_2^2}} & \frac{x_2}{\sqrt{x_1^2 + x_2^2}} & 0 \\ 0 & 0 & 1 \end{bmatrix}_{x = x^{(i)}}. \quad (27)$$

The transversal dynamics of each quadrotor in the platoon are stabilized to $\xi^{(i)} = 0$, $i = 0, 1, \ldots$, using PID controllers, while all robots except for the platoon leader implement the platoon control law (14) in their tangential dynamics. The leader is independent of the platoon, and implements an application-specific controller. The overall control scheme is shown in Fig. 3.

C. Admittance Control on Leader

Human-robot interaction is a well-suited application of TFL due to the safety provided by path constraints. An admittance controller is implemented in the tangential dynamics of the platoon leader. The controller allows the

quadrotor to change its apparent mechanical admittance so that it reacts to external forces in the same way as a mass-damper system, with user-specified values for the mass and damping coefficient. Since humans naturally expect that a mass will move when force is applied and then slow down due to friction, the admittance controller emulates an interaction analogous to a mass submerged in a viscous fluid.

Based on the approach described in [20], the admittance controller consists of two components: a reference generator and a position controller. The reference generator is responsible for creating the virtual trajectory that a mass-damper system with user-specified values would take under the influence of human-applied forces. The position controller then ensures that the quadrotor's position tracks the virtual trajectory, so that from the perspective of the interacting human, the quadrotor appears to behave with the specified mechanical properties.

1) Reference Generation: The reference signal $\eta_{\text{ref}}(t)$ is defined to be the position of the virtual mass-damper system with mass $m = 2.0\text{kg}$ and damping coefficient $b = 0.2$. Note that the actual mass of the leader quadrotor is only about 0.5kg. The dynamics of the reference signal are driven by $f_{\text{human}}(t)$, which is defined as the instantaneous force applied by the human on the platoon leader quadrotor, resulting in the following equation of motion:

$$m\ddot{\eta}_{\text{ref}}(t) + b\dot{\eta}_{\text{ref}}(t) = f_{\text{human}}(t). \tag{28}$$

Since there are no force sensors on the quadrotors, the human-applied force is estimated using a Kalman filter implemented only in the leader's tangential subsystem based on the approach taken in [20]. The force is modeled as driven entirely by Gaussian noise: $\dot{f}_{\text{human}}(t) \sim \mathcal{N}(0, \sigma_f^2)$, where σ_f^2 is a tuning parameter [20]. The leader's tangential dynamics, as given in equation (24), are augmented to include f_{human} as part of the state. The measured position of the quadrotor along the path is obtained by transforming equation (20) into path coordinates. A linear Kalman filter is then implemented with discretized versions of the augmented dynamics and measurement equation in order to estimate the human-applied force, f_{human}, at each sampling time step. Note that the resulting Kalman filter is only implemented in the leader's tangential subsystem, unlike the implementation in [20].

2) Position Tracking: The platoon leader's position along the path, $\eta^{(0)}(t)$, is controlled to track the reference signal, $\eta_{\text{ref}}(t)$, using the auxiliary control variable, $v_{\parallel}^{(0)}$. Define the error signal of the platoon leader as the difference between the reference trajectory and the leader's position along the path:

$$e^{(0)}(t) := \eta_{\text{ref}}(t) - \eta_1^{(0)}(t). \tag{29}$$

Then, the error can be stabilized with a PID controller:

$$v_{\parallel}^{(0)}(t) = k_P^{(0)} e^{(0)}(t) + k_I^{(0)} \int_0^t e^{(0)}(\tau)\mathrm{d}\tau + k_D^{(0)} \dot{e}^{(0)}(t), \tag{30}$$

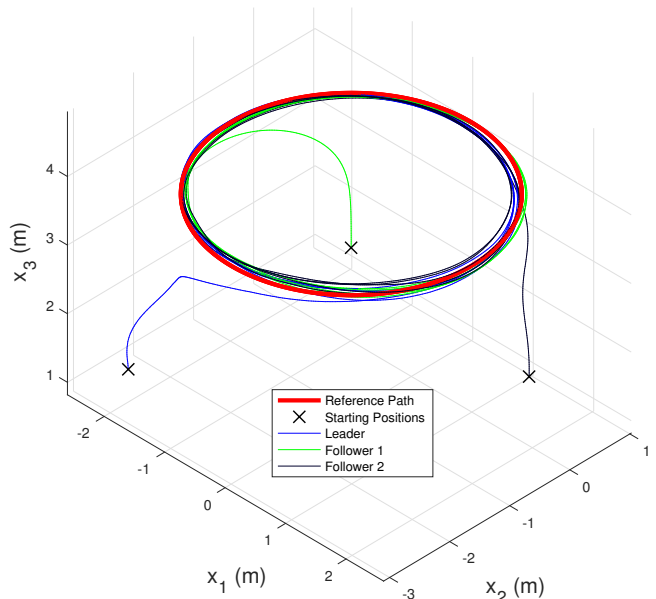where $k_P^{(0)}$, $k_I^{(0)}$, and $k_D^{(0)}$ are appropriately tuned PID gains.

Fig. 4. The flight test shows the 3D trajectories of the platoon members converging to the circle with radius 2.0m and the platoon simultaneously, while the platoon leader tracks a constant speed reference of 1.5m/s along the path. The circular path is offset 4.0m from the ground. The attractive property of the path results in asymptotic convergence, whereas the invariance property ensures every quadrotor remains on the path for all time.

Using the admittance controller, the platoon leader responds to human-applied forces analogous to a point mass in a damping medium. Simultaneously, the entire platoon is constrained to the path at all times, ensuring safety to the interacting human.

IV. EXPERIMENTAL RESULTS

A. Path and Platoon Convergence Experiment

The desired path was set as a circle of radius 2.0m at a height of 4.0m from the ground. Three quadrotors, placed arbitrarily on the ground, were used to demonstrate the simultaneous convergence of the quadrotors to the platoon formation and the platoon to the path. Note that the platoon leader did not implement the admittance controller described in subsection III-C, but rather tracked a constant speed reference of 1.5m/s along the path. Fig. 4 shows the flight paths of the quadrotors converging to the virtual path and Fig. 5 shows the tangential subsystem positions of the platoon members. Qualitative observations are that the path's invariance and attractive properties are satisfied, and that the control scheme is satisfactory.

B. Path-Constrained Human Interaction Experiment

In this experiment, the circle's height was reduced to 2.0m to allow a user to interact with the platoon leader. The leader's admittance controller was tuned to emulate the virtual mass-damper dynamics of equation (28). The lower plot in Fig. 6 shows the estimated force applied by the human and a threshold-filtered force, similar to the approach in [20]. The upper plot shows the resulting displacement along the
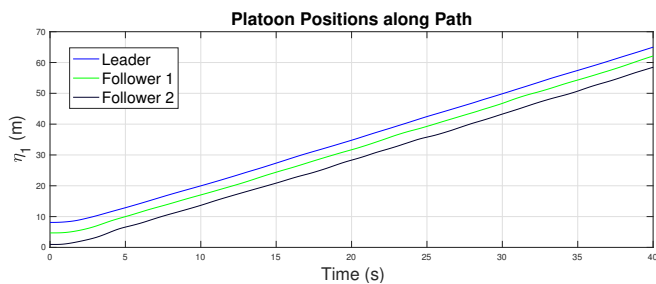
Fig. 5. The platoon leader tracks a constant velocity of 1.5m/s along the path. After the first 5s, the followers converge to the platoon and maintain their constant reference spacing of 2.5m for the duration of the experiment.
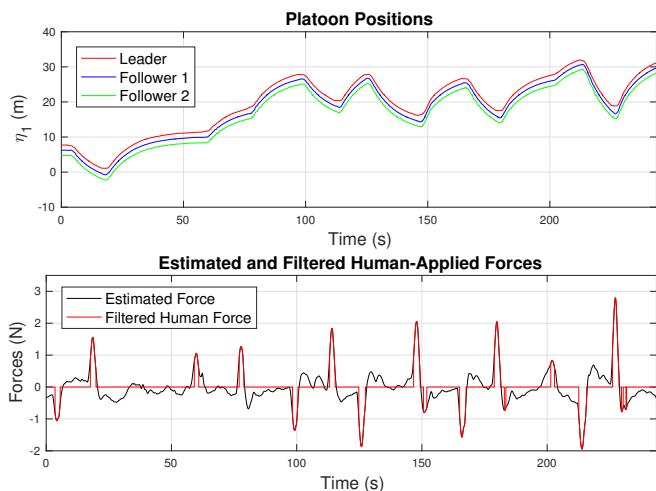

Fig. 6. In the tangential dynamics, the quadrotor platoon responds to human-applied forces. Shown in the bottom plot, the raw estimated forces are filtered to extract the human-applied forces, using the approach described in [20]. These filtered forces then drive the leader's position reference generation of equation (28), resulting in the instantaneous positions of the platoon members shown in the upper plot.

path of the quadrotors in the platoon. The constant spacing between the quadrotors demonstrates the platoon maintaining its formation while the leader responds to human-applied forces and guides the platoon.

V. CONCLUSION

This paper demonstrates how TFL simplifies the control architecture for a platoon with virtual path constraints. Stabilizing the transversal subsystem of each platoon member allows each robot to remain on the path. In the tangential subsystem, the platoon leader implements an admittance controller, while the rest of the platoon members implement platoon controllers to regulate their spacing requirements. Experiments explored human-platoon interaction, which demonstrated how the path constraints guarantee safety to the human. For future work, exploring different applications for different mechanical systems and more general paths, such as spline-interpolated paths of [10] or paths described using parallel transport frames [11], would support broader utility of platoon control with virtual path constraints.

REFERENCES

[1] S. Kumar and R. Gill, "Path following for quadrotors," IEEE Conference on Control Technology and Applications, pp. 2075–2081, 2017.
[2] C. Nielsen, C. Fulford, and M. Maggiore, "Path following using transverse feedback linearization: application to a maglev positioning system," American Control Conference, pp. 3045–3050, 2009.
[3] C. Nielsen and M. Maggiore, "On local transverse feedback linearization," SIAM Journal on Control and Optimization, vol. 47, pp. 2227–2250, 2008.
[4] R. Gill, D. Kulic, and C. Nielsen, "Robust path following for robot manipulators," IEEE/RSJ International Conference on Intelligent Robots and Systems, pp. 3412–3418, 2013.
[5] A. Hladio, C. Nielsen, and D. Wang, "Path following for a class of mechanical systems," IEEE Transactions on Control Systems Technology, pp. 2380–2390, 2013.
[6] K. J. Kazim, J. Bethge, J. Matschek, and R. Findeisen, "Combined predictive path following and admittance control," American Control Conference, pp. 3153–3158, 2018.
[7] R. Bonna and J. F. Camino, "Trajectory tracking control of a quadrotor using feedback linearization," International Symposium on Dynamic Problems of Mechanics, 2015.
[8] C. Liu, J. Pan, and Y. Chang, "PID and LQR trajectory tracking control for an unmanned quadrotor helicopter: experimental studies," Chinese Control Conference, pp. 10845–10850, 2016.
[9] A. Isidori, "Nonlinear Control Systems," Springer, 1995.
[10] R. Gill, D. Kulic, and C. Nielsen, "Spline Path Following for Redundant Mechanical Systems," IEEE Transactions on Robotics, pp. 1378–1392, 2015.
[11] B. Bischof, T. Gluck, and A. Kugi, "Combined Path Following and Compliance Control for Fully Actuated Rigid Body Systems," IEEE Transactions on Control Systems Technology, pp. 1750–1760, 2017.
[12] J. Ploeg, H. Nijmeijer, and E. V. Nunen, "Design and experimental evaluation of cooperative adaptive cruise control," IEEE Conference on Intelligent Transportation Systems, pp. 260–265, 2011.
[13] D. Swaroop and J. K. Hedrick, "Constant spacing strategies for platooning in automated highway systems," ASME Journal on Dynamic Systems, Measurement, and Control, vol. 121, pp. 462–470, 1999.
[14] D. Swaroop and J. K. Hedrick, "String stability of interconnected systems," American Control Conference, vol. 3, pp. 1806–1810, 1995.
[15] J. Ploeg, D. P. Shukla, N. van de Wouw, and H. Nijmeijer, "Controller synthesis for string stability of vehicle platoons," IEEE Transactions on Intelligent Transportation Systems, vol. 15, no. 2, pp. 854–865, 2014.
[16] L. Xiao and F. Gao, "Practical string stability of platoon of adaptive cruise control vehicles," IEEE Transactions on Intelligent Transportation Systems, vol. 12, no. 4, pp. 1184–1194, 2011.
[17] X. Liu and S. S. Mahal, "Effects of Communication Delay on String Stability in Vehicle Platoons," IEEE Transactions on Intelligent Transportation Systems, pp. 625–630, 2001.
[18] R. Rajamani and C. Zhu, "Semi-autonomous adaptive cruise control systems," IEEE Transactions on Vehicular Technology, vol. 51, no. 5, pp. 1186–1192, 2002.
[19] M. L. Della Vedova, M. Rubagotti, T. Facchinetti and A. Ferrara, "Platooning control of autonomous nonholonomic mobile robots in a human-robot coexisting environment," American Control Conference, pp. 6569–6574, 2012.
[20] F. Augugliaro and R. DAndrea, "Admittance control for physical human-quadrocopter interaction," European Control Conference, pp. 1805–1810, 2013.
[21] L. Y. Chang and H. C. Chen, "Linearization and Input-Output Decoupling for Nonlinear Control of Proton Exchange Membrane Fuel Cells," Energies, pp. 591-606, 2014.
[22] S. Lupashin, M. Hehn, M. W. Mueller, A. P. Schoellig, M. Sherback, and R. DAndrea, "A platform for aerial robotics research and demonstration: The flying machine arena," Mechatronics, vol. 24, no. 1, pp. 41-54, 2014.